

# Knowledge-Based Performance Assessment of Existing RC Buildings

FATEMEH JALAYER, LUDOVICA ELEFANTE,  
IUNIO IERVOLINO, and GAETANO MANFREDI

Department of Structural Engineering, University of Naples Federico II,  
Naples, Italy

*One of the most challenging aspects of the seismic assessment of existing buildings is the characterization of structural modeling uncertainties. Recent codes, such as Eurocode 8, seem to synthesize the effect of structural modeling uncertainties in the so-called confidence factors that are applied to mean material property estimates. The confidence factors are classified and tabulated as a function of discrete knowledge levels acquired based on the results of specific in-situ tests and inspections. In this approach, the effect of the application of the confidence factors on structural assessment is not explicitly stated. This work presents probabilistic performance-based proposals for seismic assessments of RC buildings based on the knowledge levels. These proposals take advantage of the Bayesian framework for updating the probability distributions for structural modeling parameters based on the results of tests and inspections. As structural modeling parameters, both the mechanical material properties and also the structural detailing parameters are considered. These proposals can be categorized based both on the amount of structural analysis effort required and on the type of structural analysis performed. An efficient Bayesian method is presented which relies on simplified assumptions and employs a small sample of structural model realizations and ground motion records in order to provide an estimate of structural reliability. As an alternative proposal suitable for code implementation, the simplified approach implemented in the SAC-FEMA guidelines is adapted to existing structures by employing the efficient Bayesian method. This method takes into account the effect of both ground motion uncertainty and the structural modeling uncertainties on the global performance of the structure, in a closed-form analytical safety-checking format. These alternative proposals are demonstrated for the case study structure which is an existing RC frame. In particular, it is shown how the parameters for the safety-checking format can be estimated and tabulated as a function of knowledge level, outcome of tests, and the type of structural analysis adopted.*

**Keywords** Performance-based Assessment; Existing Buildings; Bayesian Updating; Structural Modeling Uncertainties; Confidence Factor; Knowledge Levels; Reliability

## 1. Introduction

Many European countries are subjected to a considerable seismic hazard. Quite a few of these countries enjoy a rich patrimony of existing buildings, which for the most part were built before modern seismic design provisions made their way into the constructions codes. Therefore, the existing buildings can potentially pose serious fatality and economic risks in the event of a strong earthquake. A recent and unfortunate case is the L'Aquila Earthquake of April 6, 2009 in central Italy.

Received 16 September 2009; accepted 6 June 2010.

Address correspondence to Fatemeh Jalayer, Department of Structural Engineering, University of Naples Federico II, Via Claudio 21, Naples 80125, Italy; E-mail: fatemeh.jalayer@unina.it

**TABLE 1** Recommended minimum requirements for different levels of inspection and testing

KL	Inspections of reinforcement details (% structural elements)	Testing of Materials (sample/floor)
Limited	20	1
Extended	50	2
Comprehensive	80	3

One main feature distinguishing the assessment of existing buildings from that of the new construction is the large amount of uncertainty present in determining the structural modeling parameters. The recent European codes seem to provide a level of conservatism in the assessment of existing buildings, by the application of the confidence factors (CF) to mean material property estimates. These confidence factors are to be determined as a function of the knowledge levels (KL). The knowledge levels are determined based on the amount of tests and inspections performed on the building. Table 1 illustrates the three KL's, namely, limited, extended and comprehensive [CEN, 2003].

With the emerging of concepts such as *life-cycle cost analysis* and performance-based design, the question arises as to what the CF would signify and would guarantee in terms of the structural seismic reliability [Jalayer *et al.*, 2008, 2010; Franchin *et al.*, 2008]. This would not be possible without a thorough characterization of the uncertainties in the structural modeling parameters [e.g., Jalayer *et al.* 2008, 2010; Monti and Alessandri, 2008]. Another issue regards the definition of the KL: the current code definition in Table 1 leaves some room for interpretation. For example, it does not specify the spatial configuration and the outcome of the test results. Moreover, the logical connection between the numerical values for the CF's and the attainment of the KL's is not clear.

This work focuses on performance-based probabilistic proposals for the seismic assessment of existing RC structure based on different KL's. As one of the proposals, a novel and efficient simulation-based Bayesian method is presented for structural reliability assessments taking into account both the structural modeling uncertainties and the record-to-record variability in ground motion (GM). This method exploits a relatively small number of structural analyses in order to yield the *robust reliability* for the structure in question. The term *robust* herein refers to the fact that the reliability is calculated taking into account all possible structural models and their relative plausibilities [Beck and Au, 2002; Papadimitriou *et al.*, 2001].

Moreover, it is demonstrated how the efficient Bayesian method can be used in order to estimate the parameters of a simplified analytic safety-checking format arranged similar to Load-Resistance Factor Design (LRFD) for different KL's considering dynamic analyses. This format is already adopted in the American Department of Energy Guidelines DOE-1020 and in SAC-FEMA guidelines [FEMA, 2000a,b,c,d]. For seismic assessment based on static analyses, an analytical safety-checking formulation is adopted which yields the global structural response, represented by a structural performance parameter, corresponding to a certain confidence. If the parameters of these safety-checking formats (for static and dynamic analyses) are estimated for different KL's, these formats will be potentially suitable for code implementation. In this article, the standard Monte Carlo Simulation is used as a benchmark in order to verify the accuracy of the efficient Bayesian method which uses a small sample of simulations. For each KL, the outcome of tests and inspections is incorporated by employing the Bayesian updating framework. In fact, the Bayesian

framework for probabilistic inference seems to be a perfect vehicle for taking into account the results of tests and inspections in updating the structural model. In a previous work [Jalayer *et al.*, 2010], the authors demonstrated how an advanced simulation scheme (i.e., the Markov Chain Monte Carlo algorithm) can be used to both update the structural reliability and also the probability distribution for the modeling parameters based on test and inspection results. In the present work, more simple and less computationally intensive methods are investigated. A set of “multi-level” options for the analyst to choose from are proposed. By “multi-level,” multiple levels of sophistication in the method and quantity of analysis effort is intended.

### 1.1. The Structural Performance Parameter and the Structural Reliability

The structural performance parameter in this work is formatted in terms of a critical demand to capacity ratio. This parameter, denoted as  $Y$ , assumes the value of unity at the onset of the limit state  $LS$ . In the case of static analyses, the capacity spectrum method (CSM) [Fajfar, 1999] is used to obtain  $Y$ . Moreover, at the onset of the limit state, the shear capacity of the structural components is also verified by calculating the shear demand to capacity ratio for the structural components. The overall structural performance parameter is finally taken as the larger between the critical shear component demand to capacity ratio and the overall demand to capacity ratio derived from CSM. The structural reliability in the static case is expressed as the probability that  $Y$  exceeds one:

$$P_f = P(Y > 1) \quad (1)$$

In the case of dynamic analyses, the *cut-sets* concept in system reliability theory [Ditlevsen and Madsen, 1996] is employed to find the critical component demand to capacity ratio that takes the structure closer to the onset of the limit state  $LS$ . This critical demand to capacity ratio corresponds to the strongest component of the weakest structural failure mechanism [Jalayer *et al.*, 2007]:

$$Y = \min_l \max_j \frac{D_{lj}}{C_{lj}}, \quad (2)$$

where  $l$  is the structural mechanism index considered and  $j$  is the component index within the  $l^{\text{th}}$  mechanism. In this case, the mechanisms considered involve the ultimate chord rotation in the components, the formation of global mechanisms (e.g., soft story and beam mechanisms) and the component shear capacity. The structural reliability in the dynamic case is represented by the mean annual frequency (MAF) that the performance parameter  $Y$  defined in (2) exceeds unity (or simply, the MAF of failure). Taking the spectral acceleration at the fundamental period of the structure as the intensity measure, the MAF of failure can be calculated by integrating fragility and hazard for all values of spectral acceleration [Jalayer *et al.*, 2007]:

$$\lambda_f = \lambda_{Y>1} = \int P(Y > 1 | S_a) |d\lambda(S_a)| \quad (3)$$

### 1.2. The Knowledge Levels

Four distinct knowledge levels are taken into consideration in the current work. The first KL, referred to as  $KL_0$ , describes the state of the knowledge about the structure before

in-situ tests and inspections are performed. The other three KL's, namely,  $KL_1$ ,  $KL_2$ , and  $KL_3$ , are characterized based on the Eurocode 8 recommendations, *limited*, *extended*, and *comprehensive*, respectively.

**1.3. A Performance-Based Safety-Checking Format (Dynamic Analyses)**

As an alternative to the CF approach in code-based recommendations, a probabilistic and performance-based approach, adopted in the American Department of Energy Guidelines DOE-1020 and in SAC-FEMA guidelines [Cornell *et al.*, 2002], is chosen in this work. This simplified approach leads to an analytical and closed-form solution which compares the factored demand against factored capacity. The factored demand and capacity are respectively equal to median demand and capacity multiplied by some factors. The magnifying demand factors and the de-magnifying capacity factors can take into account all sources of uncertainty, such as record-to-record (ground motion) variability, structural modeling uncertainty, and the uncertainty in the capacities. This approach, also known as the Demand and Capacity Factor Design (DCFD) [Cornell *et al.*, 2002] for its similarity with the Load and Resistance Factor Design (LRFD), takes into account the overall effect of the various types of uncertainties on a global structural performance parameter:

$$\eta_Y(P_o) \cdot e^{\frac{1}{2} \frac{\kappa}{b} (\beta_{Y|S_a}^2 + \beta_{UC}^2)} \leq 1, \tag{4}$$

where  $P_o$  is an acceptable threshold for structural failure probability and  $\eta_Y(P_o)$  is the median structural performance parameter corresponding to the acceptable probability  $P_o$ .  $\kappa$  is the slope coefficient for linear regression (in the logarithmic space) of spectral acceleration hazard versus spectral acceleration and  $b$  is the slope coefficient for linear regression (in the logarithmic space) of the structural performance parameter  $Y$  vs. spectral acceleration. The terms  $\beta_{Y|S_a}$  and  $\beta_{UC}$  represent the effect of record-to-record (ground motion) variability and structural modeling uncertainties, respectively, on the total dispersion in the structural performance parameter given spectral acceleration (see Jalayer and Cornell, 2009, for more details on how to estimate  $\eta_Y(P_o)$  and  $\beta_{Y|S_a}$ ). The inequality in (4) can be verified with a certain  $x\%$  confidence:

$$\eta_Y(P_o) \cdot e^{\frac{1}{2} \frac{\kappa}{b} \beta_{Y|S_a}^2} \leq e^{-\Phi^{-1}(x) \sqrt{\beta_{Y|S_a}^2 + \beta_{UC}^2}}, \tag{5}$$

where  $\Phi^{-1}(x)$  is the inverse Gaussian cumulative distribution function (CDF) for percentile  $x$ . Note that, in this formulation, in contrast to (4), the factored demand is compared to a less than unity quantity in order to provide a certain level of confidence in the assessment, which is suitable for code implementation.

**1.4. A Performance-Based Safety-Checking Format (Static Analyses)**

In the static case, safety-checking is performed by calculating a given percentile  $x\%$  of the structural performance parameter  $Y$  and by verifying whether it is less than or equal to unity:

$$\eta_Y \cdot e^{\Phi^{-1}(x)\beta_Y} \leq 1, \tag{6}$$

where  $\eta_Y$  is the median value and  $\beta_Y$  is the standard deviation of the logarithm for the structural performance variable  $Y$ . As explained before, the percentile  $x$  reflects a desired level of confidence in the structural performance.

## 2. Methodology

In this section, the analytical basis for the methods proposed and discussed in this work is presented.

### 2.1. Characterization of the Uncertainties

It is assumed that the vector  $\theta$  represents all the uncertain parameters considered in the problem. Typically, the uncertainties present in seismic assessment can be classified in different groups, namely: (a) the uncertainties in the representation of the GM; (b) the modeling uncertainties associated with the structural finite element model; (c) the component capacity models; (d) and the uncertainties in the structural modeling parameters. It should be mentioned that since this research effort uses the code procedure involving the application of confidence factors as a point of reference, the uncertainties in the capacity models are not taken into account. This is because the Eurocode 8 takes into account the uncertainty in the capacity model separately by applying a less-than-unity safety factor  $\gamma_{ei}$ . This work focuses on the uncertainty in the structural modeling parameters related to the available information on the characteristics of existing buildings. This is the type of uncertainty that is believed to be addressed implicitly by the application of CF's. Two groups of structural modeling uncertainties are considered, the uncertainty in the mechanical property of materials and the uncertainty in the structural construction details. In particular, the structural construction details can include stirrup spacing, concrete cover, anchorage, and splice length; these are also known as the *defects*. One of the main characteristics of the construction details modeling is that possible deviations from the original configurations are mostly taken into account in those cases leading to undesirable effects. This justifies why the uncertainties related to construction details are sometimes referred to as the *defects*.

It is common to distinguish between the uncertainty that reflects the variability of the outcome of a repeatable experiment (*aleatory* uncertainty) and the uncertainty due to limited or imperfect knowledge (*epistemic* uncertainty). For instance, the strength of materials is affected by both aleatory and epistemic uncertainties; instead, the information relative to construction details is affected by epistemic uncertainties as they can be reduced with inspections. In any case, in the framework of Bayesian updating both types of uncertainty are treated in the same manner. Hence, in this work both the epistemic and aleatory uncertainties are simply referred to as uncertainties.

In order to take into account the uncertainty in the representation of the GM, a set of 30 records (listed in Appendix A) based on Mediterranean events are chosen from European Strong Motion Database (<http://www.isesd.cv.ic.ac.uk/ESD/frameset.htm>), 28 recordings, and the database of the Next Generation Attenuation of Ground Motions (NGA) Project ([http://peer.berkeley.edu/products/nga\\_project.html](http://peer.berkeley.edu/products/nga_project.html)), 2 recordings.

They are all main-shock recordings and include only one of the horizontal components of the same registration. The soil category on which the GMs are recorded is stiff soil ( $400 \text{ m/s} < V_{s30} < 700 \text{ m/s}$ ) which is consistent with the Eurocode 8 soil-type B (the soil-type for the site of the case study presented in this work). The earthquake events have moment magnitude between 5.3 and 7.2, and closest distances ranging between 7 km and 87 km (Fig. 11). Moreover, a set of seven records, recorded on stiff soil, are chosen from European Strong Motion database; they are all main-shock recordings and include only one

**TABLE 2** The uncertainties in the material properties (systematic per floor)

Material	Type	Median	COV
$f_c$	LN	165	0.15
$f_y$	LN	3200	0.08

of the horizontal components of the same registration. The earthquake events have moment magnitude between 5.4 and 6.5, and closest distances ranging between 18 and 87 km. In order to have a set compatible with the code-specified spectrum of Eurocode 8 or EC8 [CEN, 2003] the suite of records has been scaled linearly in amplitude (Fig. 9).

The parameters identifying the prior probability distributions for the material mechanical properties (concrete strength and the steel yielding force) have been based on the values typical of the post world-war II construction in Italy [Verderame *et al.*, 2001a,b]. Table 2 shows these parameters that are used to define the Lognormal probability distributions for the material properties.

The prior probability distributions for the structural detailing parameters are defined based on qualitative prior information coming from expert judgment or based on *ignorance* in the extreme case [Jalayer *et al.*, 2010]. Table 3 shows (for illustrative purpose only) the example specifications used to construct the prior probability distributions for the structural detailing parameters. Since the focus of this work is on the procedure for seismic assessment given the knowledge level, the prior probability distribution characteristics shown in Table 3 are merely for illustrative purposes. Therefore, a thorough characterization of the prior probability distributions for the structural defects is out of the scope of this work. The table shows a list of possible defects, their probability distribution and correlation characteristics. For the construction details regarding the steel rebar, the uncertain parameter is a less-than-unity factor which will be applied to the steel area. That is why the maximum value for the uncertain parameters related to longitudinal rebar defects is equal to unity.

## 2.2. Updating the Probability Distributions

The probability distributions for the structural modeling parameters are updated employing the Bayesian framework for inference. It is assumed that the material properties are homogeneous across each floor or construction zone. Therefore, the material property value assigned to each floor can be thought of as an average of the material property values across the floor in question. The results of tests and inspections for each floor are used to update the probability distribution for the mean material property across the floor. Figure 1 illustrates an example where the test results for concrete strength have all verified the nominal value ( $f_c = 165 \text{ Kg/cm}^2$ ,  $16.18 \text{ N/mm}^2$ ) for different levels of knowledge. It is observed that the updated curve has the same median but has its dispersion reduced as the amount of data increases. In the following, the updating procedure for the concrete strength  $f_c$  is demonstrated; the exact same procedure is applied also for updating the probability distribution for steel yielding strength  $f_y$ .

Let  $\mathbf{d} = \{d_i : i = 1 : N\}$  denote the set of data available for the concrete strength for a given construction zone. Assuming that the data measurements contain no errors, the updated probability distribution for mean concrete strength across the floor can be calculated using the Bayes formula:

$$p(f_c|\mathbf{d}) = \frac{p(\mathbf{d}|f_c)p(f_c)}{\int p(\mathbf{d}|f_c)p(f_c)df_c} \quad (7)$$

**TABLE 3** The uncertainties in structural detailing parameters

Defects	Possibilities	Prob.	Type
Insufficient anchorage (Beams)	sufficient (100% effective) absent (50% effective)	Uniform [0.50,1]	Systematic over floor
Error in diameter (Columns)	$\phi_{16}$ $\phi_{14}$	Uniform [0.7697,1]	Systematic over floor and section type
Superposition (Columns)	100% of the area effective 75% of the area effective	Uniform [0.75,1]	Systematic over floor
Errors in configuration (columns)	More plausible configuration Less plausible configuration	Uniform [0.75,1] [0.67,1]	Systematic over floor and section type
Absence of a bar (beams)	Absence of a bar Presence of a bar	Uniform [0.70,1] [0.69,1] [0.60,1]	Systematic over floor and section type
Stirrup spacing	Uniform (beams)	Uniform [15 cm, 30 cm]	Systematic
Stirrup spacing	Uniform (beams)	Uniform [20 cm, 35 cm]	Systematic
Spacing of shear rebar	Uniform (column)	Uniform [20 cm, 35 cm]	Systematic

Assuming that the data are independent, the likelihood  $p(\mathbf{d}|f_c)$  is written as:

$$p(\mathbf{d}|f_c) = \prod_{i=1}^N p(d_i|f_c), \quad (8)$$

where  $p(f_c)$  denotes the prior probability distribution for the mean concrete strength across the construction zone. For example, in this case it can refer to the characterization of the uncertainty in concrete strength, before the tests are conducted, for the knowledge level  $KL_0$ ; that is the Lognormal distribution described in Table 2. The likelihood functions,  $p(d_i|f_c)$ , are also assumed to be Lognormal probability distributions with median value equal to  $f_c$  and standard deviation of the logarithm equal to the value tabulated in Table 2. Figure 1 illustrates the probability distribution of the mean concrete strength value across the construction zone for the knowledge levels —  $KL_0$ ,  $KL_1$ ,  $KL_2$ , and  $KL_3$  — based on the extreme hypothesis that all the test results confirm the nominal value. It should be mentioned that this hypothesis is considered for the purpose of parameter studies on the effect of test results. Otherwise, the methodology is general with respect to the outcome of the test results. It is observed from the figure that standard deviation for the updated



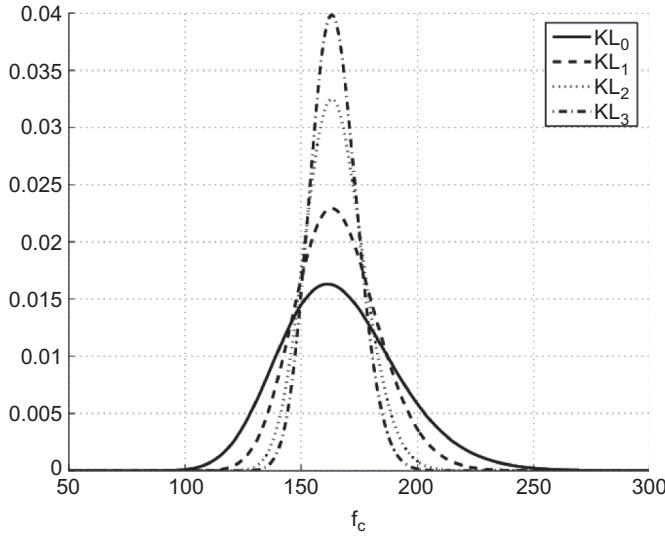


**FIGURE 1** The prior and the updated probability distributions for concrete strength for different knowledge levels.

probability distribution for each KL decreases across increasing knowledge levels while the median value remains invariant.

With regard to the structural detailing parameters, a slightly different approach is employed. Assuming that the probability of not having a construction defect in a member is equal to  $f$ , the probability distribution for  $f$  is updated using the test results. If the test results indicate that out of  $n$  cases observed  $n_d$  of them demonstrate a defect, the probability distribution for  $f$  is also updated according to the Bayes formula:

$$p(f|\mathbf{d}) = \frac{p(\mathbf{d}|f)p(f)}{\sum_f p(\mathbf{d}|f)p(f)}, \tag{9}$$

where  $p(f)$  is the prior probability distribution for  $f$  and  $p(\mathbf{d}|f)$  is the likelihood function for the data  $\mathbf{d}$  given the value of  $f$ . In the absence of prior information it is assumed that  $p(f)$  is an uniform distribution from 0 to 1. Use can be made of expert judgment in order to limit the lower and the upper bounds for the defect probability.

The likelihood function is calculated using the binomial distribution:

$$p(\mathbf{d}|f) = \binom{n}{n_d} (1-f)^{n_d} f^{n-n_d} \tag{10}$$

which gives the probability of having exactly  $n_d$  successes out of  $n$  trials. In relation to the structural detailing parameters, this model is adopted assuming that the number of trials corresponds to the number of inspections of the reinforcement detail in question, expressed in terms of % of the structural elements for each KL (Table 1). The number of successes, instead, corresponds to the outcomes of inspections, for example whether they verify the nominal value or not. In this work, three different hypotheses are considered regarding the outcome of the simulated inspections, that is:

1. 100% of the inspections verify the design values indicated in the original documents;



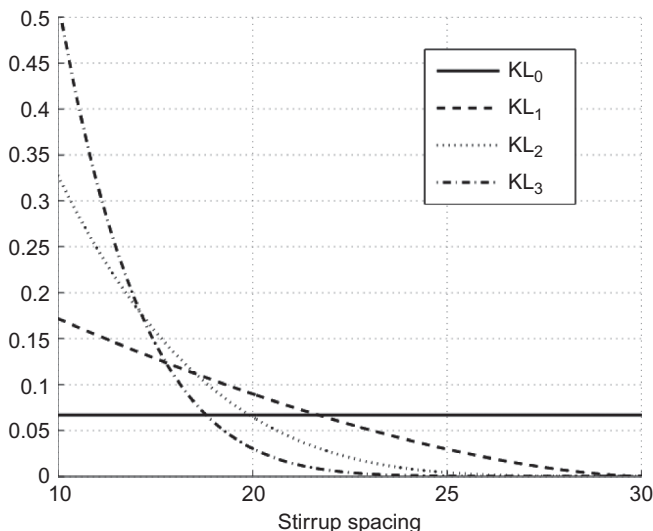


**FIGURE 2** The uniform prior and updated probability distributions for the spacing of the shear stirrups.

2. 50% of the inspections verify the design values indicated in the original documents;
3. 0% of the inspections verify the design values indicated in the original documents.

Figure 2 illustrates the prior probability distribution for the spacing between the shear reinforcement together with updated distribution based on the hypothesis that all of the test results verify the design value ( $s = 15$  cm). It is observed that the consideration of the test data focuses more narrowly the probability distribution around the design value. Figure 3 displays the prior distribution for the anchorage effectiveness factor. The figure also shows the updated probability distributions after the test results for the three KL's verify the design value (i.e., effectiveness factor equal to unity). The same as the probability distribution for stirrup spacing, it is observed that, across the increasing KL's, the probability distributions become more and more focused around the nominal value. The nominal value is taken as the value indicated in the original design documents if available.

### 2.3. An Efficient Method for Estimation of Robust Reliability

Suppose that the probability of failure is described by an analytical probability distribution with parameters  $\chi = (\eta_Y, \beta_Y)$  (e.g., median and standard deviation of the Lognormal distribution). If the probability of failure given the set of parameters is denoted by  $P(F|\chi)$ , the expected value (or the robust estimate) for the probability of failure for a given set of data values  $\mathbf{d} = \{d_i : i = 1 : N\}$  is expressed as:

$$E[P(F|\mathbf{d})] = \int_{\Omega} P(F|\chi)p(\chi|\mathbf{d})d\chi, \quad (11)$$

where  $p(\chi|\mathbf{d})$  is the posterior probability distribution for the set of parameters  $\chi$  given the data  $\mathbf{d}$  and  $\Omega$  is the space of possible values for  $\chi$ . The robust variance for the probability of failure is calculated as:

$$\sigma_{P(F|\mathbf{d})}^2 = E[P(F|\mathbf{d})^2] - E[P(F|\mathbf{d})]^2 \quad (12)$$

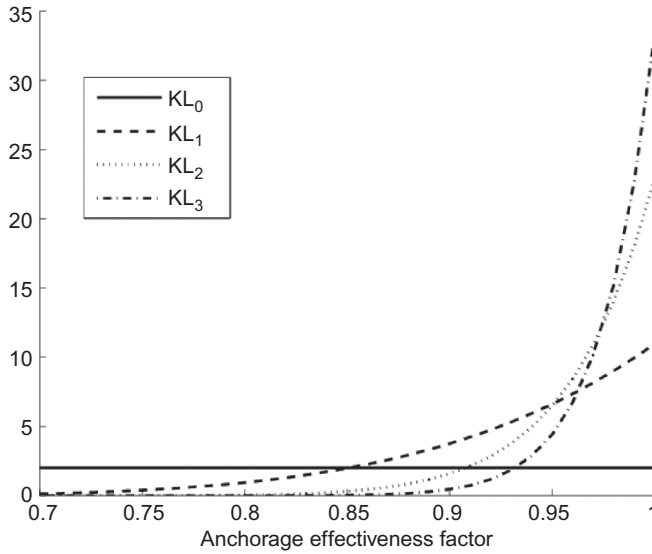


**FIGURE 3** The uniform prior and the updated probability distributions for the anchorage effectiveness factor.

In particular, if the dataset  $\mathbf{d}$  is expressed in terms of a set of  $Y$  values calculated for different realizations of the uncertain parameters within the problem, the structural reliability or the probability of failure in the case considering structural modeling uncertainties (given the code-specified spectrum) can be expressed by a Lognormal complementary cumulative distribution function (CCDF) as following  $\chi = \{\eta_Y, \beta_Y\}$ :

$$P(Y(\underline{\theta}) > 1) = 1 - \Phi\left(\frac{-\log \eta_Y}{\beta_Y}\right), \tag{13}$$

where  $\Phi$  is the Gaussian CDF,  $Y$  is the structural performance index, and  $\eta_Y$  and  $\beta_Y$  are the median and the standard deviation (of the logarithm) for the probability distribution of the structural performance index. Using the Bayesian updating framework, the posterior probability distribution for median and standard deviation based on data  $Y$  is written as [Box and Tiao, 1992]:

$$P(\eta_Y, \beta_Y | Y) = k \beta_Y^{-(n+1)} \exp\left(-\frac{\nu s^2 + n(\log \eta_Y - \overline{\log Y})^2}{2\beta_Y^2}\right) \tag{14}$$

$$k = \sqrt{\frac{n}{2\pi}} \left(\frac{\Gamma(\nu/2)}{2}\right)^{-1} \left(\frac{\nu s^2}{2}\right)^{\nu/2},$$

where  $Y = \{Y_1, \dots, Y_n\}$  is the vector of  $n$  different realizations of the structural performance index,  $k$  is a normalizing constant,  $\Gamma(\cdot)$  is the gamma function,  $\nu = n - 1$ ,  $\overline{\log Y}$  is the sample mean value for  $\log Y$ , and  $\nu s^2$  is sum of the squares of the deviations from the sample mean value. The expected value and standard deviation for the probability of failure are calculated from Eqs. (11) and (12) based on the posterior probability distribution  $p(\eta_Y, \beta_Y | Y)$  in (14). Otherwise, the best-estimate values for the median and standard

deviation can be calculated either as the maximum likelihood pair for the posterior probability distribution function in (14) or the contour corresponding to a given (e.g., 84%) confidence level.

In the dynamic case, the structural fragility as a function of spectral acceleration in the presence of modeling uncertainties and uncertainties in the representation of the GM can be calculated from the following Lognormal CCDF:

$$P(Y(\underline{\theta}) > y|S_a) = 1 - \Phi \left( \frac{\log y - \log \eta_{Y|S_a}}{\beta_{UT}} \right) \quad (15)$$

$$\beta_{UT}^2 = \beta_{Y|S_a}^2 + \beta_{UC}^2,$$

where  $\eta_{Y|S_a}$  is the median for the probability distribution of the structural performance index and  $\beta_{UT}$  is the total standard deviation for the probability distribution of the structural performance index including the contribution from record-to-record variability and the overall effect of the structural modeling uncertainties. The terms  $\beta_{Y|S_a}$  and  $\beta_{UC}$  represent the effect of the uncertainty in the GM representation and the uncertainty in the material properties and the structural details, respectively. It should be noted that (15) yields the structural fragility; after integrating it with the hazard function for the spectral acceleration, the MAF that the structural performance variable  $Y$  exceeds a specific value or the structural risk curve is obtained.

Suppose that a selection of  $n$  ground motion records are used to represent the effect of GM uncertainty on the structural performance index. Let  $S_{a,i}$  and  $Y_i$  represent the spectral acceleration and the performance index for the GM record  $i$ , respectively. The posterior probability distribution for standard deviation is calculated as:

$$P(\beta_{UT}|Y) = \left[ \frac{1}{2} \Gamma \left( \frac{\nu}{2} \right) \right]^{-1} \left( \frac{\nu s^2}{2} \right)^{\frac{\nu}{2}} \beta_{UT}^{-(\nu+1)} \exp \left( \frac{-\nu s^2}{2\beta_{UT}^2} \right) \quad (16)$$

The data pairs  $(Y, S_a)$  are gathered by calculating  $Y$  for the set of  $n$  GM records applied to the structural model generated by different realizations of material mechanical properties and structural detailing parameters.  $\nu$  is the degrees of freedom and is equal to  $n - 2$ ,  $\nu s^2$  is equal to the sum of the square of the residuals for a linear regression of  $\log Y$  on  $\log S_a$ , and  $a$  and  $b$  are the regression coefficients. The joint posterior probability distribution for the coefficients of the linear regression  $\omega = (\log a, b)$  are calculated as:

$$P(\omega|Y, S_a) = k \left[ \frac{1 + (\omega - \hat{\omega})^T \mathbf{X}^T \mathbf{X} (\omega - \hat{\omega})}{\nu s^2} \right]^{-\frac{n}{2}} \quad (17)$$

$$k = \frac{\Gamma(\frac{n}{2}) \sqrt{n \sum \log S_{a,i}^2 - (\sum \log S_{a,i})^2}}{\nu s^2 \Gamma(\frac{1}{2})^2 \Gamma(\frac{n}{2} - 1)}$$

which is a *bivariate t-distribution* where  $\mathbf{X}$  is a  $n \times 2$  matrix whose first column is a vector of ones and its second column is the vector of  $\log S_{a,i}$ ,  $\omega$  is the  $2 \times 1$  vector of regression coefficients  $\log a$  and  $b$ , and  $\hat{\omega}$  is the vector  $(\log a, b)$  of the coefficients of the linear regression of structural performance parameter  $Y$  vs.  $S_a$  in the logarithmic space (due to record-to-record variability only). The median and the standard deviation for the probability distribution for  $Y|S_a$  are taken equal to the maximum likelihood estimates  $\eta_{Y|S_a} = a S_a^b$

and  $\beta_{Y|S_a} = s$ , that is, the conditional median value for  $Y$  is estimated by a power-law function of  $S_a$  and the conditional standard deviation (of the logarithm) of  $Y$  given  $S_a$  is assumed to be constant. The robust estimates for the expected value and the standard deviation of the failure probability are obtained from (11) and (12) based on the product of the posterior probability distributions  $p(\omega|Y, S_a)$  and  $p(\beta_{UT}|Y, S_a)$  in (16) and (17), assuming they are independent  $\chi = (\omega, \beta_{UT}) = (\log a, b, \beta_{UT})$ .

#### 2.4. Estimating the Parameters of the Analytic Safety-Checking Formats

The previous sub-section lays out an efficient Bayesian method for calculating the structural reliability for different KL's taking into account both the structural modeling uncertainties and the uncertainty due to record-to-record variability. This sub-section discusses how the SAC-FEMA safety-checking format and the confidence interval formulation described in Secs. 1.3 and 1.4 are modified and how their corresponding parameters can be estimated using the efficient Bayesian method.

In the static case, the formulation in (6) for obtaining the  $x$  percentile of the structural performance parameter is re-written as follows:

$$\hat{Y} \cdot \gamma \cdot e^{\Phi^{-1}(x)\beta_Y} \leq 1, \tag{18}$$

where  $\gamma$  is a bias factor and  $\beta_Y$  is the standard deviation of the robust fragility curve.  $\hat{Y}$  represents the structural performance parameter calculated for the structural model corresponding to the median material properties based on the test results and nominal values for the structural detailing parameters. The bias factor  $\gamma$  represents the (usually larger-than-unity) factor that once multiplied by the nominal value  $\hat{Y}$  leads to the median value  $\eta_Y$ . Comparing with (6),  $\gamma$  can be calculated as:

$$\gamma = \frac{\eta_Y}{\hat{Y}} \tag{19}$$

Likewise, when the uncertainty in the GM representation is considered, the formulation in (5) can be re-written as:

$$\hat{Y} \cdot \gamma \cdot e^{\frac{1}{2} \frac{k}{b} \beta_{Y|S_a}^2} \leq e^{-\Phi^{-1}(x) \sqrt{\beta_{Y|S_a}^2 + \beta_{UC}^2}}, \tag{20}$$

where  $\gamma$  is a bias factor and  $\beta_{UC}$  represent the over-all effect of structural modeling uncertainties.  $\hat{Y}$  represents the structural performance parameter calculated based on the median material properties obtained from the test results and nominal values for the structural detailing parameters. For instance,  $\hat{Y}$  can be calculated by performing linear least squares as a function of the first-mode spectral acceleration based on the set of records. The bias factor  $\gamma$  represents the (usually larger-than-unity) factor that once multiplied by the nominal value  $\hat{Y}$  leads to the median value  $\eta_Y(P_o)$  for the structural performance parameter for an admissible probability value  $P_o$ :

$$\gamma = \frac{\eta_Y(P_o)}{\hat{Y}}, \tag{21}$$

where  $\eta_Y(P_o) = a \cdot S_a(P_o)^b$  using the maximum likelihood estimates of regression coefficients ( $\log a, b$ ) obtained from the probability distribution in (17) (i.e., the  $\omega = (\log a, b)$  vector that maximizes  $P(\omega|Y, S_a)$ ),  $S_a(P_o)$  is calculated as the spectral acceleration

value corresponding to a MAF of exceedance equal to  $P_o$  on the spectral acceleration hazard curve.

### 3. Numerical Example

As the case study, an existing school structure located in Avellino (Italy) is considered herein. The structure is situated in seismic zone II according to the former Italian seismic guidelines [OPCM 3431, 2005]. The structure consists of three stories and a semi-embedded story and its foundation lies on soil type B. For the structure in question, the original design notes and graphics have been gathered. The building is constructed in the 1960's and it is designed for gravity loads only, as it is frequently encountered in the post second World War buildings.

In Fig. 4a, the tri-dimensional view of the structure is illustrated; it is observed that the building is irregular both in plane and elevation. In order to reduce the computational effort, the main central frame in the structure is extracted and used as the structural model (Fig. 4b). The columns have rectangular section with the following dimensions: first story  $40 \times 55 \text{ cm}^2$ ; second story  $40 \times 45 \text{ cm}^2$ ; third story  $40 \times 40 \text{ cm}^2$ ; and fourth story  $30 \times 40 \text{ cm}^2$ . The beams, also with rectangular section, have the following dimensions:  $40 \times 70 \text{ cm}^2$  at first and second story, and  $30 \times 50 \text{ cm}^2$  for the upper two floors. It is inferred from the original design notes that the steel re-bar is of the type Aq42 and the concrete has a minimum resistance equal to  $165 \text{ kg/cm}^2$  ( $16.18 \text{ N/mm}^2$ ) [Regio Decreto Legge, 1939]. The finite element model of the frame is constructed assuming that the nonlinear behavior in the structure is concentrated in plastic hinges located at the element ends. Each beam or column element is modeled by coupling in series of an elastic element and two rigid-plastic hinges. The rigid-plastic element is defined by its moment-rotation relation which is derived by analyzing the reinforced concrete section at the hinge location. In this study, the section analysis is based on (the widely adopted in current practice) Mander-Priestly [Mander *et al.*, 1988] constitutive relationship for reinforced concrete, assuming that the concrete is not confined, and the reinforcing steel behavior is elastic-perfectly-plastic. The behavior of the plastic hinge is characterized by four phases, namely: rigid, cracked, post-yielding, and post-peak. In addition to flexural deformation, the yielding rotation takes into account also the shear deformation and the deformation related to bar-slip based on the code recommendations [OPCM 3431, 2005]. Moreover, the shear span used in the calculation of

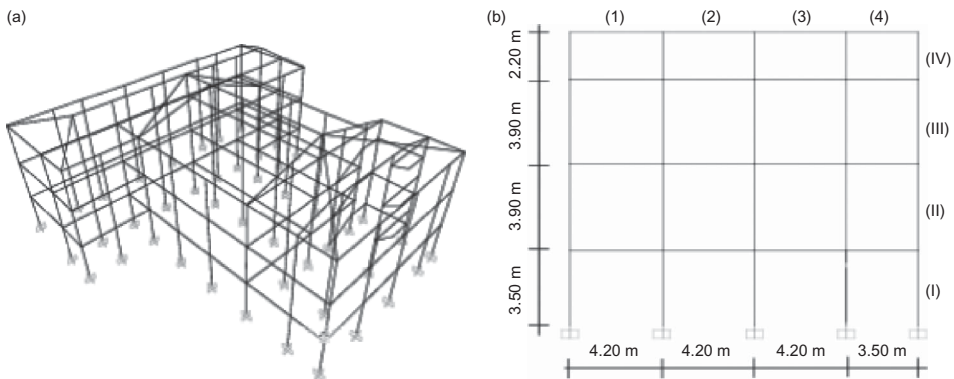


**FIGURE 4** (a) The 3-D structural model and (b) the central frame extracted for performing the analyses.

the plastic rotation is based on the code formulas. As it relates to the post-peak behavior, it is assumed that the section resistance drops to zero with a post-peak negative slope. The structural analyses are performed using the Open System for Earthquake Simulation (OpenSees, <http://opensees.berkeley.edu/index.php/>).

### 3.1. The Structural Performance Index: Static Analyses

When only the structural modeling uncertainties are considered, the definition of structural capacity in this work is based on the limit state of significant damage, as proposed by Eurocode 8. That is, the onset of critical behavior in the first element, characterized by member chord rotations larger than  $3/4^{\text{th}}$  of the corresponding ultimate chord rotation capacity. The structural demand is characterized by the intersection of the code-based inelastic design spectrum and the static pushover curve transformed into that of the equivalent single degree of freedom system. As an index for the global structural performance, the ratio of structural demand to capacity is used. The component shear failure demand to capacity ratios are also considered; the shear capacity for each component is calculated using the procedure based the truss action caused by a variable fracture angle. The obtained results are combined with the CSM demand to capacity using the *cut-set* concept of the system reliability theory in order to find the critical demand to capacity ratio  $Y$  which takes the structure closer to the onset of the limit state.

### 3.2. Calculating the Structural Fragility Using the Efficient Bayesian Method: Static Analyses

The structural fragility curve for the structure under study is calculated by employing the efficient Bayesian method described before based on  $Y$  for static analyses for a set of 20 Monte Carlo (MC) realizations of the structural model. These realizations take into account the uncertainties in the material properties and the structural defects (as listed in Tables 2 and 3). The probability distributions for the uncertain parameters are updated according to the increasing KL's. Thus, for each knowledge level, the 20 realizations of the structural model are generated from the (updated) probability distributions corresponding to the KL's (as described in Sec. 2.2) and based on the results of in-situ tests and inspections. Since the results of tests and inspections actually available for the frame in question did not exactly match the Eurocode 8 definition of the KL's (Table 1), the test and inspection results used herein are simulated assuming that all the results verify the design values indicated in the original documents. Figure 5 demonstrates the robust fragility curves (the probability of failure for a given value of  $Y$ ) obtained. The robust fragility for knowledge levels  $KL_1$ ,  $KL_2$ , and  $KL_3$  is calculated from (11) as the expected value of the structural fragility in (13), given that its median and standard deviation are known, where the joint probability distribution for median and standard deviation is given in (14). For each KL, the standard deviation in the robust fragility estimate is calculated from (12) as a measure of the error in the estimation of the structural reliability using the efficient Bayesian method.

It is observed from Fig. 5 that upon increasing KL's both the median and the dispersion in the fragility curves ( $\beta_Y$  and  $\eta_Y$  in [13]) decrease assuming that the test and inspection results all verify the nominal values. However, it can be immediately observed that the structure does not verify the confidence-based safety-checking criteria in (1) in any of the KL's. That is, because the median  $\eta_Y$  is already greater than unity. This is due to the fact that the structural components do not verify against shear, a typical problem for existing reinforced concrete structures not designed for seismic loading. Figure 6 shows the plus/minus one standard deviation confidence interval for the robust fragility curves

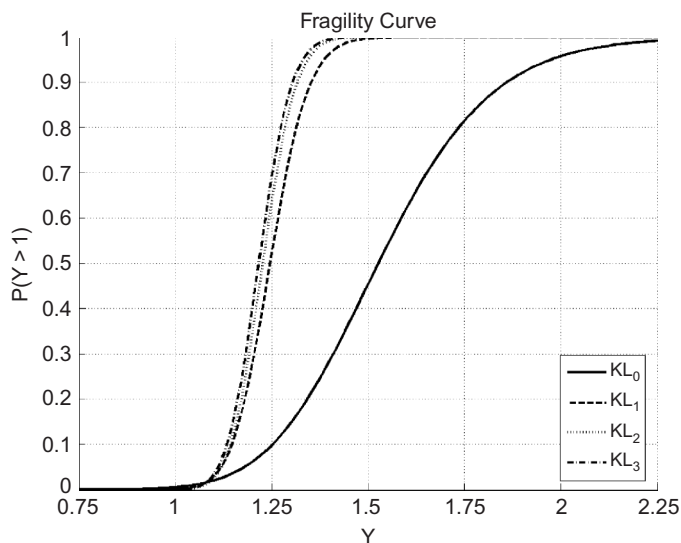


**FIGURE 5** The structural fragility curves for the knowledge levels  $KL_0$ ,  $KL_1$ ,  $KL_2$ , and  $KL_3$ .

for each KL together with the structural performance parameter obtained applying the CFs specified in the code for each KL (the vertical lines). An alternative probability-based definition of the CF is used herein, based on the global performance of the structure, by the CF leading to a structural performance parameter that has a specific (say 95%) probability of not being exceeded. The horizontal lines in the figure illustrate the 95% confidence level and the star indicates the structural performance parameter that has 95% probability of not being exceeded. Comparing this alternative confidence-based definition to the values obtained by applying the code procedure for knowledge levels  $KL_1$ ,  $KL_2$ , and  $KL_3$ , it is observed that, for this case study example, the two definitions agree reasonably well and that the code-based values are slightly conservative (keeping in mind however, that the 95% level is chosen arbitrarily).

The robust fragility curves and their corresponding plus/minus standard deviation confidence intervals are also obtained based on two alternative hypotheses with respect to the original hypothesis in which all the tests and inspections verify the nominal values. The first hypothesis states that none of the test results confirm the nominal value and the second hypothesis states that only 50% of the test results verify the nominal value. The resulting robust fragility curves are shown in Fig. 7 for the three KL's. It is observed that the standard deviation for the fragility curves remains more-or-less invariant with respect to the test results while the median value significantly changes. Obviously, these hypotheses, assuming that the percentage of not verifying the test results is constant for all the tests and inspections performed, are quite simplified with respect to the reality.

### 3.3. Verification of Results Using the Standard Monte Carlo Simulation (MCS)

The standard Monte Carlo Simulation is used as a benchmark for verifying the accuracy of the efficient Bayesian method described in Secs. 2.3 and 3.2 for the static case. The fragility curve for the prior knowledge level  $KL_0$  is obtained using 500 Monte Carlo simulations.



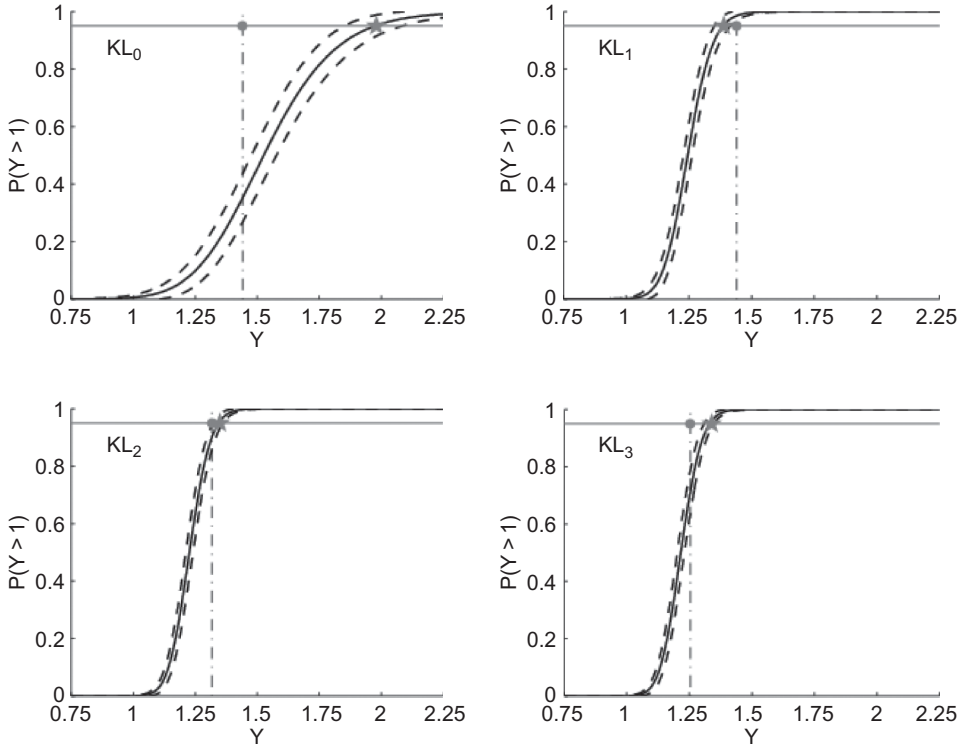


**FIGURE 6** The plus/minus standard deviation interval structural fragility curves for the knowledge levels  $KL_0$ ,  $KL_1$ ,  $KL_2$ , and  $KL_3$ .

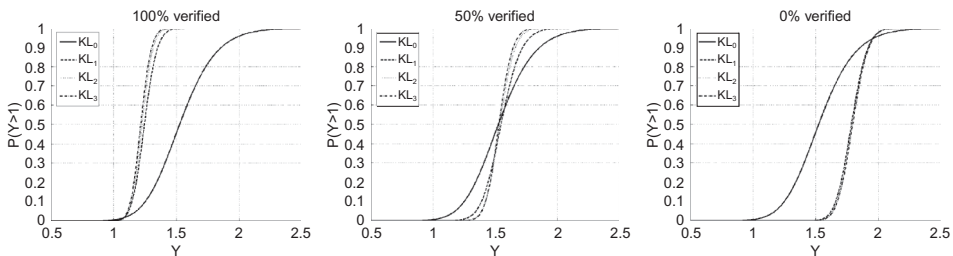


**FIGURE 7** The structural fragility curves for the knowledge levels  $KL_0$ ,  $KL_1$ ,  $KL_2$ , and  $KL_3$  corresponding to different percentages of the construction detail inspections verifying the nominal values.

For knowledge levels  $KL_1$ ,  $KL_2$ , and  $KL_3$ , the fragility curves are obtained using 200 simulations (given the reduced dispersion in the corresponding updated probability distributions for  $KL_1$ ,  $KL_2$ , and  $KL_3$  with respect to  $KL_0$ , less simulations were necessary in order to obtain the fragility curve). It should be noted that the number of samples generated in the Monte Carlo simulations is limited due to the fact that the failure probability  $P(Y > 1|KL)$  is almost unity. In other words, the failure zone can be simulated with less simulations. For very rare events (small failure probabilities), a Monte Carlo simulation procedure may involve around thousands of analyses.

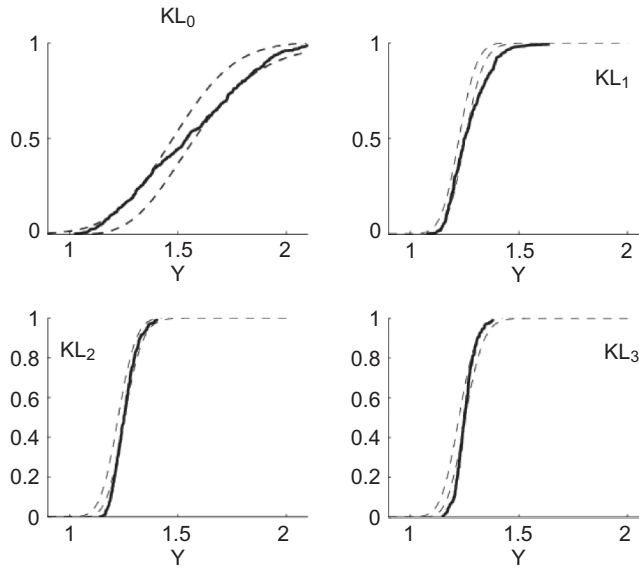


**FIGURE 8** Comparison between the plus/minus standard deviation interval structural fragility curves obtained with the efficient Bayesian method and the fragility curves calculated based on MCS for the knowledge levels  $KL_0$ ,  $KL_1$ ,  $KL_2$ , and  $KL_3$ .

Figure 8 illustrates that the plus/minus one standard deviation fragility curves obtained by the efficient Bayesian method agree well with MCS results.

### 3.4. The CF Method for Considering the Structural Modeling Uncertainty: Dynamic Analyses

Section 3.2, Fig. 6, shows how applying the CF's can affect the overall structural performance using the nonlinear static analyses. In a similar way, this section shows how applying CF's can influence the structural performance using the nonlinear dynamic analysis. A set of seven GM records described in more detail in Sec. 2.1 are chosen. In order to have a set compatible with the code-specified spectrum (EC8), the suite of records has been scaled. In Fig. 9, the scaled spectra with corresponding scaled factors are plotted. For each KL specified in the code, the structural performance variable for the set of records is calculated for a structural model (without defects) with material properties divided by the corresponding CF. The structural performance variable  $Y$ , calculated for each GM record, as described Sec. 1.1 from (2), is related to the spectral acceleration using linear regression with parameters  $\eta_{Y|Sa}$  and  $\beta_{Y|Sa}$ ; that is, the conditional median and standard deviation of logarithm of the structural performance parameter given spectral acceleration, respectively. The structural fragility is calculated from (15) setting  $\beta_{UC}$  equal to zero. Finally, the structural fragility is integrated with the hazard curve for spectral acceleration at the fundamental period of the structure equal to 0.75 s (extracted from the official Italian seismic hazard at <http://esse1.mi.ingv.it/d3.html> for the coordinates of the site lat. 40.915 and lon. 14.78) in order to calculate the mean annual probability of exceeding a specific value of  $Y$ . The resulting curves corresponding to different values of CF are plotted in Fig. 10. As mentioned in Sec. 1.1, the MAF that the performance parameter  $Y$  exceeds unity serves as a measure of structural reliability in the case of dynamic analyses.

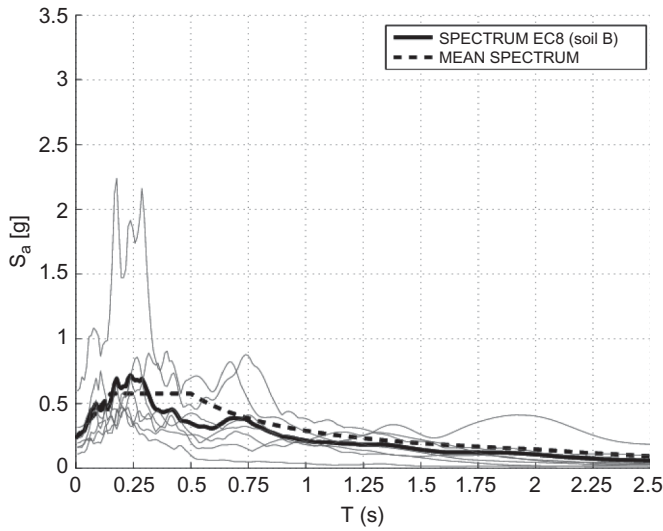


**FIGURE 9** Scaled acceleration spectra (7 GM records). The ground motion records are all scaled by a factor of 1.50 except for one (Umbria-Marche) that is scaled by 3.50.

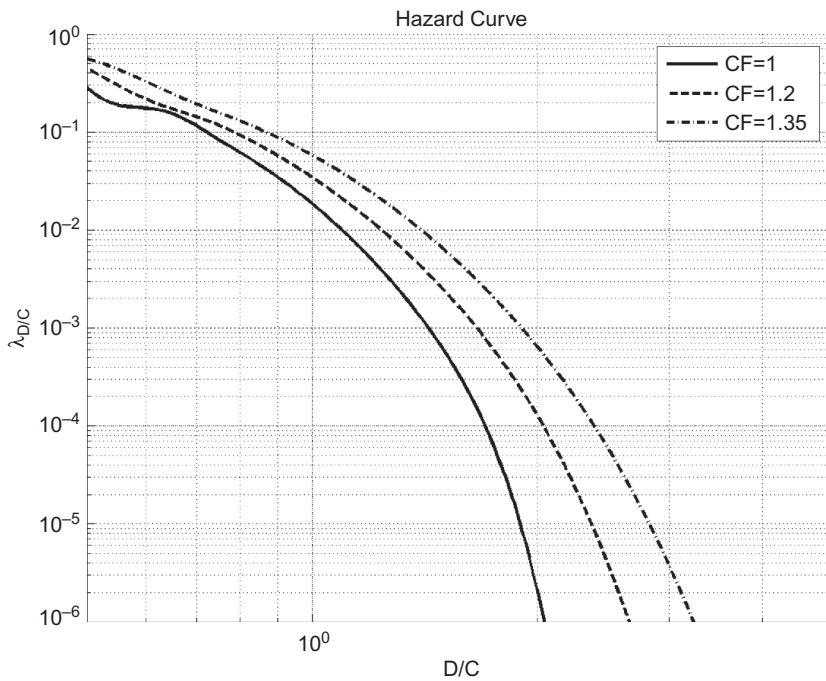


**FIGURE 10** Seismic risk curves obtained following the CF approach for knowledge levels  $KL_0$ ,  $KL_1$ ,  $KL_2$ , and  $KL_3$ .

**3.5. Calculating the Structural Reliability Using the Efficient Bayesian Method: Dynamic Analyses**

The curves of the MAF of exceeding a given value of  $Y$  (or more concisely, the seismic risk curves) for increasing levels of knowledge are calculated in this stage by integrating

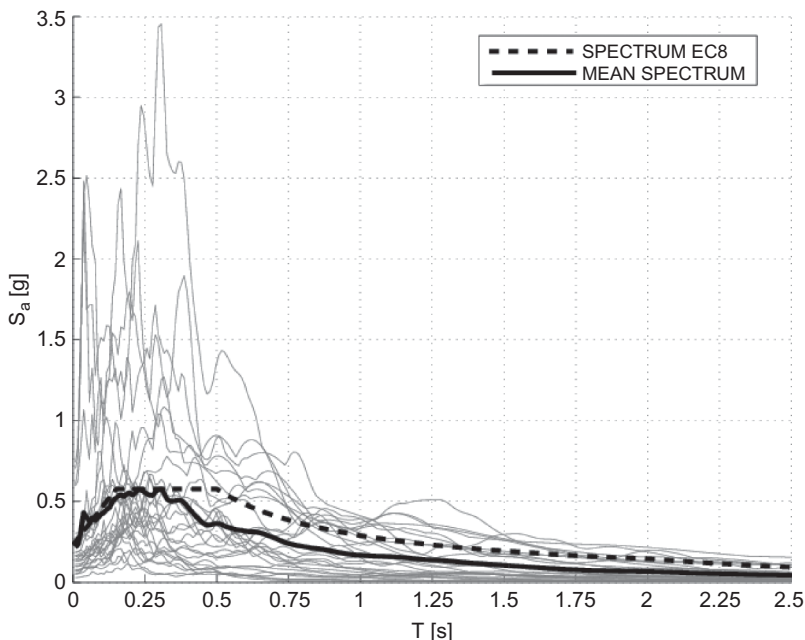


**FIGURE 11** Acceleration spectra (30 records, unscaled).

the robust fragilities, obtained from the efficient Bayesian method, and the spectral acceleration hazard curve at the site of the structure. For each KL, the robust fragility is calculated from (11), (15), (16), and (17) using a set of 30 MC realizations of the structural model. The conditional median,  $\eta_{Y|S_a}$ , and standard deviation of the logarithm,  $\beta_{Y|S_a}$ , for the structural performance parameter  $Y$  are estimated by employing the linear least squares of natural logarithm of  $Y$  as a function of the natural logarithm of spectral acceleration at the fundamental mode of the structure. The joint probability distribution for the linear least squares coefficients  $\omega = (\log a, b)$  is calculated from (17). The probability distribution for the standard deviation of the fragility curve  $\beta_{UT}$  (related to  $\beta_{Y|S_a}$  and  $\beta_{UC}$  through [15]) is calculated from (16) based on the results of a small set of 30 Monte Carlo simulations. The standard deviation as it is seen in (15) can be calculated as the square root of the sum of squares of two parts representing the effect of GM uncertainty denoted by  $\beta_{Y|S_a}$  and the structural modeling uncertainty denoted by  $\beta_{UC}$ .

The set of MC realizations for each KL are generated based on the corresponding (updated) probability distributions. The suite of 30 records described in Sec. 2.1 are used (Fig. 11, Appendix A).

The resulting seismic risk curves are plotted in solid lines in Fig. 12 for knowledge levels  $KL_0$ ,  $KL_1$ ,  $KL_2$ , and  $KL_3$ . For each KL, the curve obtained by following the code procedure and applying the corresponding CF is plotted in dashed lines. The horizontal line in each sub-figure represents the allowable probability level, here taken as 10% probability of exceedance in 50 years. It is observed that for an acceptable probability of  $P_o = 0.002$  or 10% in 50 years, the structure does not meet the safety criterion  $Y < 1$  (i.e., the MAF of failure in (3) is greater than the acceptable probability level  $P_o$ ) for any of the KL. The intersection of the admissible level with the risk curves obtained using the CF method and the risk curves obtained using the efficient Bayesian method are shown with circles and stars, respectively. It is observed, that for this case study, there is very good agreement between

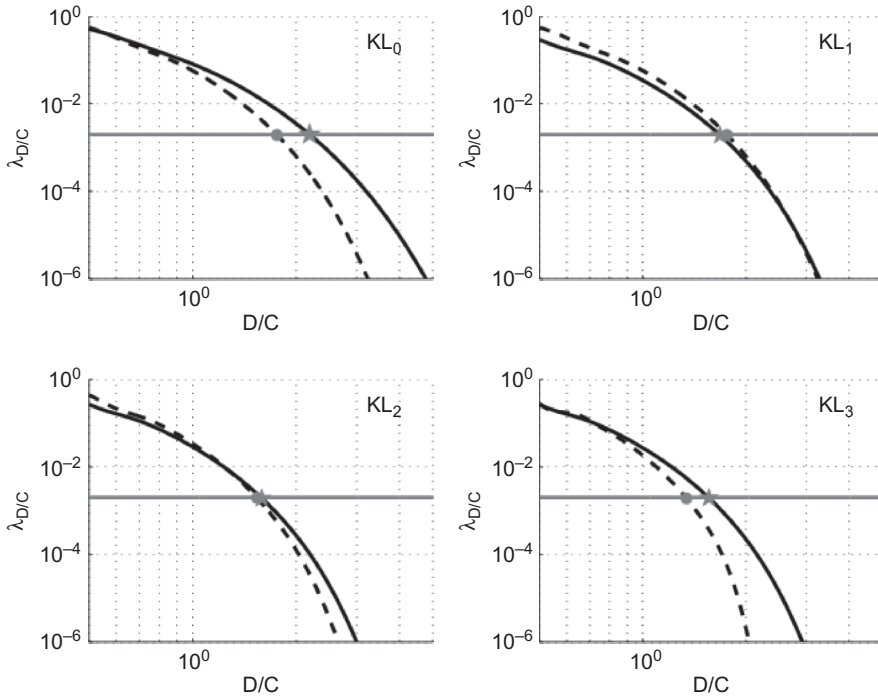


**FIGURE 12** The seismic risk curves obtained from the efficient Bayesian method (solid lines) and the seismic risk curves obtained based on the CF approach (dashed lines) for knowledge levels KL<sub>0</sub>, KL<sub>1</sub>, KL<sub>2</sub>, and KL<sub>3</sub>.

the CF results and those of the efficient Bayesian method for KL<sub>1</sub> and KL<sub>2</sub>. However, the CF results are on the unconservative side for KL<sub>0</sub> and KL<sub>3</sub>. These results are particularly interesting since they benchmark the code-based CF method with a probabilistic method in which the effect of both structural modeling uncertainty and the record-to-record variability are explicitly taken into account.

### 3.6. Estimating the Parameters of the Performance-Based Safety-Checking Formats Using the Efficient Bayesian Method

The fragility curves calculated for both the static and dynamic case using the efficient Bayesian method can be used in order to estimate the parameters of the analytical safety-checking formats discussed beforehand. For the static case, the bias factor  $\gamma$  is calculated from (19) and the standard deviation  $\beta_Y$  is calculated from the fragility curve obtained employing the efficient Bayesian method as half of the logarithm of the ratio of the 84<sup>th</sup> and 16<sup>th</sup> percentiles. Tables 4 and 6 outline the parameters  $\beta_Y$  and  $\gamma$  values for the three KL's considered for the case study structure and based on static analyses. The three columns represent the three simplified hypotheses adopted previously regarding the outcome of the test results. Table 7 outlines these parameters for the knowledge level KL<sub>0</sub> before the tests are performed. It is observed that the  $\beta_Y$  values remains quasi-invariant with respect to the hypotheses regarding the outcome of the tests and inspections. However, they reduce as the knowledge level increases. For instance, for KL<sub>0</sub>,  $\beta_Y$  is close to 15% which means that based on the prior distributions considered herein, considering the structural modeling

**TABLE 4** Table of values for  $\beta_{UC}$  (uncertainty in the material properties and in the structural details)

	100% verified	50% verified	0% verified
SPO			
KL <sub>1</sub>	0.0641	0.0835	0.0586
KL <sub>2</sub>	0.0527	0.0616	0.0556
KL <sub>3</sub>	0.0531	0.0554	0.0527
DYN			
KL <sub>1</sub>	0.0800	0.0868	0.1142
KL <sub>2</sub>	0.0393	0.0635	0.0742
KL <sub>3</sub>	0.0216	0.0472	0.0682

**TABLE 5** Table of values for  $\beta_{UT}$  (includes the uncertainty in the material properties, the uncertainty in the structural details, and the uncertainty in the ground motion representation)

	100% verified	50% verified	0% verified
DYN			
KL <sub>1</sub>	0.1784	0.1816	0.1938
KL <sub>2</sub>	0.1643	0.1717	0.1759
KL <sub>3</sub>	0.1609	0.1663	0.1735

**TABLE 6** Table of values for the bias factor  $\gamma$ 

	100% verified	50% verified	0% verified	CF
SPO				
KL <sub>1</sub>	0.9933	1.2343	1.4255	<b>1.35</b>
KL <sub>2</sub>	0.9782	1.2272	1.4294	<b>1.20</b>
KL <sub>3</sub>	0.9701	1.2206	1.4349	<b>1.00</b>
DYN				
KL <sub>1</sub>	1.0984	1.3306	1.4698	<b>1.35</b>
KL <sub>2</sub>	1.0521	1.3046	1.4812	<b>1.20</b>
KL <sub>3</sub>	1.0362	1.2632	1.4953	<b>1.00</b>

uncertainties influences the structural reliability up to 15%. The values for  $\beta_Y$  reduce to 5% for KL<sub>3</sub>. The bias factor  $\gamma$  remains more-or-less invariant with respect to the KL; however, it changes as a function of the percentage of the test and inspection results that verify the nominal value. For example,  $\gamma$  is approximately equal to 1.40, 1.20 and 1.0 for percentages verified equal to 100%, 50% and 0%, respectively.

The observation that  $\beta_Y$  depends on the KL unlike the bias factor  $\gamma$  that remains more-or-less invariant, is somehow to be expected. That is, given a fixed percentage of the inspections results that verify the nominal values, the increase in knowledge level (i.e., the increase in the total number of inspections) is expected to reduce the dispersion in the structural performance parameter  $Y$ . On the other hand, the bias factor is expected to depend on the number of inspections that verify rather than the total number of inspections.

**TABLE 7** Table of values for  $KL_0$ 

		$\gamma$	$\beta_{UC}$
SPO	$KL_0$	1.5245	0.1455
DYN	$KL_0$	1.3342	0.1783

For the dynamic case, the parameters for the safety-checking format in (20) are also calculated by employing the efficient Bayesian method. The bias factor  $\gamma$  is calculated from Eq. (21). The total standard deviation  $\beta_{UT} = \sqrt{\beta_{UC}^2 + \beta_{Y|S_a}^2}$  is calculated from the robust fragility curves obtained from the efficient Bayesian method as half of the logarithm of the ratio of the percentiles 84<sup>th</sup> and 16<sup>th</sup>, respectively. The standard deviation  $\beta_{Y|S_a}$  is estimated as the square root of the mean of the squared residuals of the regression of  $\log Y$  versus  $\log S_a$  without considering the structural modeling uncertainties (for the structural model constructed based on the median value of the test results for material properties and the nominal values for construction details). Hence, the value for  $\beta_{UC}$  is calculated as  $\beta_{UC} = \sqrt{\beta_{UT}^2 - \beta_{Y|S_a}^2}$ . Tables 4 and 6 tabulate the  $\gamma$  and  $\beta_{UC}$  for different KL's and test outcomes based on nonlinear time-history analyses. The same coefficients for the knowledge level  $KL_0$  are listed separately in Table 7. It is observed that the value for  $\beta_{UC}$  reduces with increasing the KL; that is,  $\beta_{UC}$  is close to 18% for  $KL_0$  and it reduces to 2% for  $KL_3$  (when 100% of the results verify) and 7% (when 0% of the results verify). The bias factor  $\gamma$  which is observed to be more-or-less invariant with respect to the KL, is approximately equal to 1.50, 1.30, and 1.0 for 0%, 50%, and 100% of the test and inspections verifying the nominal tests and inspections. Table 5 outlines the estimates for  $\beta_{UT}$  for the dynamic case for knowledge levels  $KL_1$ ,  $KL_2$ , and  $KL_3$  for different percentages of the test and inspection results verifying. It is observed that  $\beta_{UT}$  decreases a small amount (19% to 16%) with the increasing KL. The small variation in  $\beta_{UT}$  is attributed to the fact that it includes also the dispersion  $\beta_{Y|S_a}$  due to record-to-record variability. Since the value of  $\beta_{UC}$  (around 2–11%, depends on the KL and the percentage of the inspections verified) is small with respect to  $\beta_{Y|S_a}$  (around 16%, by definition depends neither on the KL nor on the percentage of the test results verified), the resulting  $\beta_{UT}$  values in Table 5 show little sensitivity to the KL.

It is emphasized that the values tabulated herein depend, in addition to being case study specific, on the simplifying assumption regarding the outcome of the test results and the assumptions regarding the prior probability distributions. However, they represent an example where given the structure, the type of analysis and the outcome of the tests and inspections, the parameters of the safety-checking formats in Sec. 2.4 are calibrated.

In perspective, with regard to possible code implementations, similar tables can be obtained by characterizing the representative building types for a given location and their period of construction. The tabulated parameters can be potentially used within the safety-checking formats discussed in this work, in lieu of thorough case-specific assessments, for performance-based assessment of existing buildings.

#### 4. Conclusions

Quantifying the uncertainty in the structural modeling parameters, related to the level of knowledge about an existing structure, is one of the main challenges in seismic performance assessment of existing buildings. The discrete knowledge levels (KL) defined by the current European codes for the performance assessment of existing buildings leave some room for interpretation and they do not lead to a unique configuration of tests and inspections.



Moreover, it is not clear which level of structural reliability does the application of the confidence factors guarantee. Hence, with the emerging of performance-based design and life-cycle cost analysis in earthquake engineering, there is need for code-based methods that map the different knowledge levels for an existing building to the global structural performance and the structural reliability.

This work proposes two alternative methods for the performance assessment of existing buildings. An efficient simulation-based Bayesian method is presented which estimates the expected value and the standard deviation for the structural fragility (static case) and the MAF of exceeding the structural performance parameter (dynamic case) with relatively small number of structural analyses ( $N = 20 - 30$ ). It is observed, upon comparison with the standard Monte Carlo simulation results, that the efficient simulation-based method provides sufficiently accurate plus/minus one standard deviation intervals for the structural fragility in the static case. As a proposal for possible code implementations, the parameters (a bias factor and a dispersion parameter) for the analytical probabilistic safety-checking format adopted in the SAC-FEMA guidelines (known as the demand and capacity factor design, DCFD) for dynamic analyses and the confidence interval formulation for the static case are estimated using the efficient Bayesian method for the case study structure. Once the bias factor and the dispersion parameter are estimated, these safety checking formats can be used for evaluating the performance of an existing building, with a certain confidence, based on only one analysis (i.e., the result of code-based procedure for  $CF = 1$ ). Table 8 provides a synthesis of these two proposals and their advantages/disadvantages. For the sake of comparison, these methods are compared in Table 8 with the standard Monte Carlo simulation at one extreme as the most computationally demanding method (e.g., number of analyses  $N = 200 - 10000$ ) and the code-based CF method ( $N = 1$ ) at the other.

The methods proposed herein characterize the uncertainty in the structural modeling parameters such as mechanical material properties and the construction detailing parameters by probability distributions. For each KL, the probability distributions for the uncertain parameters are updated using the Bayesian updating framework. In the absence of test results abiding exactly with the code prescriptions, an idealized situation is considered in which all of the test results verify the original design values. Obviously, the methodology presented is general with respect to the outcome of the test and inspections. The uncertain parameters are divided into groups (emulating various construction zones). It is assumed that the uncertain parameter belonging to distinct groups are fully un-correlated and only the uncertain parameters inside a given group can be correlated. It should be noted that decisions on possible groupings of the uncertain parameters may affect significantly the global performance assessment of the structure.

For the case study structure examined in this work, the code-based CF method can lead in some cases (depending on both the KL and the percentage of the inspections verifying the nominal values) to un-conservative results with respect to the efficient Bayesian method proposed herein, for both static and dynamic analyses. Obviously, these observations are case-specific and cannot be generalized.

As a final note relative to the case study building considered, it should be mentioned that the critical value for the structural performance variable is almost always governed by the shear failure in structural components. This is a typical problem for the existing reinforced concrete structures designed only for the gravity loads.

In perspective, the probability-based analytical safety-checking formats calibrated for the case study building herein, are potentially suitable candidates for implementation in the guidelines for existing buildings. It should be mentioned that in order to make accurate performance assessments, the best way to approach would be to carry out case-specific assessments based on the outcome of the tests and inspections. However, the

**TABLE 8** Alternative methods discussed in this paper for seismic assessment of existing buildings

Methods	Features	Advantages	Disadvantages
Standard Monte Carlo (SMC)	<ul style="list-style-type: none"> <li>• SMC simulation method employed inside the Bayesian probabilistic framework.</li> <li>• Takes into account explicitly the sources of uncertainty.</li> </ul>	<ul style="list-style-type: none"> <li>• Performance-based</li> <li>• The most accurate</li> </ul>	<ul style="list-style-type: none"> <li>• Requires many (200–10,000) structural analyses.</li> </ul>
Efficient Bayesian Method	<ul style="list-style-type: none"> <li>• A small-sample simulation method inside the Bayesian probabilistic framework.</li> <li>• Takes into account record-to-record variability based on a set of real ground motions.</li> </ul>	<ul style="list-style-type: none"> <li>• Performance-based.</li> <li>• Very efficient (20–30 analyses).</li> <li>• Provides a plus/minus standard deviation interval for the structural reliability.</li> </ul>	<ul style="list-style-type: none"> <li>• Is based on a given analytic form for the fragility curve (i.e., Lognormal)</li> <li>• Less accurate with respect to standard SMC.</li> </ul>
Analytical safety-checking formats	<ul style="list-style-type: none"> <li>• Identified by a bias factor and a dispersion parameter suitable for code implementation.</li> <li>• These parameters can be estimated using more accurate methods such as the efficient Bayesian or SMC simulation.</li> </ul>	<ul style="list-style-type: none"> <li>• Performance-based</li> <li>• Extremely efficient. Only 1 analysis for static cases; <math>\geq 7</math> analyses for dynamic cases.</li> <li>• Can establish a level of confidence for the performance assessment.</li> </ul>	<ul style="list-style-type: none"> <li>• Is based on a series of simplifying assumptions.</li> <li>• Its wide-spread use requires drafting of tables for the bias factor and the dispersion parameter for different representative classes of existing structures.</li> </ul>
Confidence Factor	<ul style="list-style-type: none"> <li>• Actual code approach (EC8, NTC) based on the application of the CF's to mean material properties values obtained by in-situ testing.</li> </ul>	<ul style="list-style-type: none"> <li>• Only 1 analysis for static cases; <math>\geq 7</math> analyses for dynamic cases.</li> </ul>	<ul style="list-style-type: none"> <li>• Less accurate compared to the two previous methods.</li> <li>• Is not performance-based.</li> <li>• Its accuracy is not known.</li> <li>• The definition of knowledge level leave a lot of room for interpretation.</li> </ul>

probability-based analytical safety-checking formats and their tabulated parameters can offer significant improvements in the assessments with respect to the current CF approach; they can serve as a less-than-ideal, approximate solution with a rigorous basis.

## Acknowledgments

This work was supported in part by the project *ReLUIS 2005/2008 – Dipartimento della Protezione Civile*. This support is gratefully acknowledged. Any opinions, findings, and conclusions or recommendations expressed in this material are those of the authors and do not necessarily reflect those of the *ReLUIS*. The valuable collaboration of the undergraduate student Fabio Petruzzelli is gratefully acknowledged.

## References

- AISC [1994] *Manual of Steel Construction Load and Resistance Factor Design*, 2nd ed., American Institute of Steel Construction Inc., Chicago, IL.
- Beck, J. L. and Au, S. K. [2002] “Bayesian updating of structural models and reliability using Markov Chain Monte Carlo simulation,” *Journal of Engineering Mechanics* **128**(4), 380–391.
- Box, G. E. P. and Tiao, G. C. [1992] *Bayesian Inference in Statistical Analysis*, Wiley Interscience, John Wiley & Sons, Inc.
- CEN, European Committee for Standardisation TC250/SC8/ [2003] *Eurocode 8: Design Provisions for Earthquake Resistance of Structures, Part 1.1: General rules, seismic actions and rules for buildings*, PrEN1998-1.
- Cornell, C. A., Jalayer, F., Hamburger, R. O., and Foutch, D. A. [2002] “The probabilistic basis for the 2000 SAC/FEMA steel moment frame guidelines,” *ASCE Journal of Structural Engineering* **128**(4), 526–533.
- Department of Energy (DOE) [1994] *Natural Phenomena Hazards Design and Evaluation Criteria for Department of Energy Facilities*, DOE-STD-1020-94, U.S. Department of Energy, Washington, D.C.
- Ditlevsen, O. and Madsen, H. [1996] *Structural Reliability Analysis*, John Wiley, New York.
- Fajfar, P. [1999] “Capacity spectrum method based on inelastic demand spectra,” *Earthquake Engineering and Structural Dynamics* **28**(9), 979–993.
- Federal Emergency Management Agency (FEMA) [2000a] *Recommended Seismic Design Criteria for New Steel Moment-Frame Buildings*, FEMA-350, SAC Joint Venture, Washington, D.C.
- Federal Emergency Management Agency (FEMA) [2000b] *Recommended Seismic Evaluation and Upgrade Criteria for Existing Welded Steel Moment-Frame Buildings*, FEMA-351, SAC Joint Venture, Washington, D.C.
- Federal Emergency Management Agency (FEMA) [2000c] *Recommended Post-Earthquake Evaluation and Repair Criteria for Welded Steel Moment-Frame Buildings*, FEMA-352, SAC Joint Venture, Washington, D.C.
- Federal Emergency Management Agency (FEMA) [2000d] *Pre-Standard and Commentary for the Seismic Rehabilitation of Buildings*, FEMA 356, Washington, D.C.
- Franchin, P., Pinto, P. E., and Pathmanathan, R. [2008] “Assessing the adequacy of a single confidence factor in accounting for epistemic uncertainty,” *Convegno RELUIS: Valutazione e riduzione della vulnerabilità sismica di edifici esistenti in cemento armato*, Roma 29–30 maggio (in Italian).
- Jalayer, F. and Cornell, C. A. [2009] “Alternative nonlinear demand estimation methods for probability-based seismic assessments,” *Earthquake Engineering and Structural Dynamics* **38**(8), 951–972.
- Jalayer, F., Elefante, L., Iervolino, I., and Manfredi, G. [2009b] “Small-sample Bayesian inference for estimation of structural modeling uncertainty parameters in seismic assessment of existing RC buildings,” *Proceedings of the ICOSSAR09 Conference*, The 10th International Conference on Structural Safety and Reliability, September 13–17, Osaka, Japan, 2272–2278.

- Jalayer, F., Franchin, P., and Pinto, P. E. [2007] “A scalar decision variable for seismic reliability analysis of RC frames,” Special issue of *Earthquake Engineering and Structural Dynamics on Structural Reliability* **36**(13), 2050–2079.
- Jalayer F., Iervolino I., and Manfredi G. [2008] “Aggiornamento Bayesiano dei parametri di modellazione strutturale e dell’affidabilità sismica dei edifici esistenti in C.A.,” Convegno RELUIS: *Valutazione e riduzione della vulnerabilità sismica di edifici in cemento armato*, Roma 29–30 Maggio 2008 (in Italian).
- Jalayer, F., Iervolino, I., and Manfredi, G. [2010] “Structural modeling uncertainties and their influence on seismic assessment of existing RC structures,” *Structural Safety* **32**(3), 220–228.
- Monti, G. and Alessandri, S. [2008] “Confidence factors for concrete and steel strength,” Convegno RELUIS: *Valutazione e riduzione della vulnerabilità sismica di edifici esistenti in cemento armato*, Roma 29–30 Maggio 2008 (in Italian).
- Ordinanza del Presidente del Consiglio dei Ministri (OPCM) n. 3431 [2005] “*Ulteriori modifiche ed integrazioni all’ordinanza del Presidente del Consiglio dei Ministri n. 3274 del 20 marzo 2003*,” Gazzetta Ufficiale della Repubblica Italiana n. 107 del 10-5-2005 (Suppl. Ordinario n. 85, in Italian).
- Ordinanza del Presidente del Consiglio dei Ministri (OPCM) n. 3519 [2006] “*Criteri per l’individuazione delle zone sismiche e la formazione e l’aggiornamento degli elenchi delle medesime zone*,” Gazzetta Ufficiale della Repubblica Italiana n. 108 (in Italian).
- Papadimitriou, C., Beck, J. L., and Katafygiotis, L. S. [2001] “Updating robust reliability using structural test data,” *Probabilistic Engineering Mechanics* **16**(2), 103–113.
- Regio Decreto Legge (R.D.L.) 2229 [1939] “*Norme per l’esecuzione delle opere in conglomerato cementizio semplice o armato*,” 1939 (in Italian).
- Verderame, G. M., Manfredi, G., and Frunzio G. [2001a] “Le proprietà meccaniche dei calcestruzzi impiegati nelle strutture in cemento armato realizzate negli anni ‘60”, X Congresso Nazionale “*L’Ingegneria Sismica in Italia*”, Potenza-Matera 9–13 Settembre (in Italian).
- Verderame, G. M., Stella, A., and Cosenza, E. [2001b] “Le proprietà meccaniche degli acciai impiegati nelle strutture in cemento armato realizzate negli anni ‘60”, X Convegno Nazionale “*L’Ingegneria Sismica in Italia*”, Potenza e Matera 9–13 Settembre (in Italian).

### Appendix A: The 30 Ground Motion Records Used in the Efficient Bayesian Method

A set of 30 ground motion records are chosen compatible with the spectrum of Eurocode 8 or EC8 [CEN, 2003].

Record	$M_w$	Fault mechanism	Vs30 [m/s]	ED [km]	FD [km]	PGA [g]	$S_a(T_1)$ [g]
Valnerina	5.8	normal	?	23	21	0.04	0.03
Friuli, Italy-02	5.9	reverse	412	18	18	0.21	0.08
Preveza	5.4	thrust	?	28	7	0.14	0.10
Umbria	5.6	normal	546	19	19	0.21	0.02
Lazio Abruzzo	5.9	normal	?	36	28	0.07	0.05
Etolia	5.3	thrust	405	20	12	0.04	0.01
Kyllini	5.9	strike slip	490	14	11	0.15	0.15
Irpinia, Italy-01	6.9	normal	600	15	18	0.13	0.30
Potenza	5.8	strike slip	494	28	29	0.10	0.08
Ano Liosia	6.0	normal	411	20	9	0.16	0.06
Adana	6.3	strike slip	?	39	30	0.03	0.05
South Iceland	6.5	strike slip	?	15	10	0.21	0.13
Patras	5.6	strike slip	665	30	?	0.05	0.02
Friuli	6.5	thrust	?	42	34	0.06	0.22
Campano Lucano (o.c.1)	6.9	normal	472	48	33	0.11	0.25
Campano Lucano (o.c.1)	6.9	normal	529	16	13	0.16	0.31
Kalamata (o.c.1)	5.9	normal	486	10	0	0.22	0.48
Kalamata (o.c.1)	5.9	normal	399	11	0	0.24	0.48

Umbria Marche (o.c.1)	6.0	normal	546	11	1	0.52	0.56
Umbria Marche	6.0	normal	450	38	27	0.09	0.17
South Iceland (o.c.1)	6.5	strike slip	?	7	6	0.63	0.54
Duzee I (o.c.1)	7.2	oblique	662	26	13	0.13	0.18
Friuli	6.5	thrust	?	87	71	0.07	0.12
Campano Lucano (o.c.2)	6.9	normal	472	48	33	0.14	0.26
Campano Lucano (o.c.2)	6.9	normal	529	16	13	0.18	0.31
Kalamata (o.c.2)	5.9	normal	486	10	0	0.30	0.63
Kalamata (o.c.2)	5.9	normal	399	11	0	0.27	0.51
Umbria Marche (o.c.2)	6.0	normal	546	11	1	0.46	0.64
South Iceland (o.c.2)	6.5	strike slip	?	7	6	0.51	0.74
Duzee I (o.c.2)	7.2	oblique	662	26	13	0.16	0.14